Steel and Composite Structures, *Vol. 27, No. 3 (2018) 273-283*
DOI: https://doi.org/10.12989/scs.2018.27.3.273

Geometrically nonlinear analysis of sandwich beams under low velocity impact: analytical and experimental investigation

Sattar Jedari Salami [*1] and Soheil Dariushi [2a]

[1] *Department of Mechanical Engineering, Damavand branch, Islamic Azad University, Damavand, Iran*
[2] *Department of Composite, Iran polymer and petrochemical Institute, Tehran-Karaj highway, Pajuhesh Boulevard, Tehran, Iran*

(*Received August 9, 2017, Revised December 29, 2017, Accepted March 3, 2018*)

Abstract. Nonlinear low velocity impact response of sandwich beam with laminated composite face sheets and soft core is studied based on Extended High Order Sandwich Panel Theory (EHSAPT). The face sheets follow the Third order shear deformation beam theory (TSDT) that has hitherto not reported in conventional EHSAPT. Besides, the two dimensional elasticity is used for the core. The nonlinear Von Karman type relations for strains of face sheets and the core are adopted. Contact force between the impactor and the beam is obtained using the modified Hertz law. The field equations are derived via the Ritz based applied to the total energy of the system. The solution is obtained in the time domain by implementing the well-known Runge-Kutta method. The effects of boundary conditions, core-to-face sheet thickness ratio, initial velocity of the impactor, the impactor mass and position of the impactor are studied in detail. It is found that each of these parameters have significant effect on the impact characteristics which should be considered. Finally, some low velocity impact tests have been carried out by Drop Hammer Testing Machine. The contact force histories predicted by EHSAPT are in good agreement with that obtained by experimental results.

Keywords: sandwich beam; low velocity impact; high order sandwich theory; nonlinear analysis; Ritz method

1. Introduction

With increasing use of sandwich structures in aerospace, automotive, naval and civil applications, a large number of researches have been carried out on the behavior of these structures. Sandwich panels usually consist of three layers, i.e., two face sheets and one core. The materials used for face sheets conventionally include thin, stiff and strong sheets of metallic or fibrous composite materials. The thick and commonly low density core materials may be foam, honeycomb or corrugated core (Caliri *et al*. 2016, Zenkert 1995, Yan and Song 2016, Ganapathi *et al*. 2016). To date, lots of theories and models have been presented and developed to explain impact behaviour of sandwich structures (Benbakhti *et al*. 2016, Bennai *et al*. 2015, Daniel *et al*. 2009). For predicting contact-force relation, the dynamics of both the impactor and the sandwich panel must be modelled accurately. In modelling the sandwich structures, several choices need to be made. In some cases, by considering the hypothesis of quasi-static behaviour, the structure models using spring-mass models. In more detailed dynamic model cases, the structure can be modelled using beam/plate/shell theory, or 2D/3D elasticity theory (Abrate and Di Sciuva 2017). Noor *et al*. (1996) divided the modelling approaches that has been used for analysis of sandwich panels to four categories: detailed models, 3D continuum models, 2D plate and shell models, and simplified models.

In addition, experimental study on mechanical properties of sandwich structures has received great attention. The experimental investigation is convenient and effective to get basic resources for further analysis.

St-Pierre *et al*. (2015) investigated the low velocity impact response of simply supported sandwich beams with corrugated and Y-frame core in a drop weight apparatus. The specimens represented 1:20 scale versions of ship hull designs. The results show that the corrugated and Y-frame core beams had similar performance. Reddy and Sharma (2014) studied the behavior of sandwich panels that comprises of silk-cotton wood skins and aluminum honeycomb core under quasi static and low velocity impact loading. The results show that the energy absorption capacity of cellular sandwich panels increases under dynamic loading in comparison with the quasi static loading conditions.

The effect of high temperature exposure on the low velocity impact behavior and damage mechanisms of composite pyramidal truss core sandwich plate were investigated experimentally by Liu *et al*. (2014) Impact test results have shown that high temperature exposure has significant influence on the absorbed energy, damage mechanisms and maximum impact force. Stocchi *et al*. (2014) made a novel honeycomb core with natural fiber reinforced composite consisting of jute fiber and vinylester matrix. The effective elastic properties of the core were calculated with a homogenization analysis and FE modeling.

*Corresponding author, Assistant Professor, E-mail: sattar.salami@aut.ac.ir
[a] Assistant Professor, E-mail: s.dariushi@ippi.ac.ir

http://www.techno-press.org/?journal=scs&subpage=6 ISSN: 1229-9367 (Print), 1598-6233 (Online)

Performance of sandwich panels consisting of PVC or aluminum foam core with aluminum skins was investigated under low velocity impact by Rajaneesh *et al*. (2014). Also, numerical models were used to predict the impact response and failure modes.

The concepts, assumptions and capabilities of the main sandwich panel theories have been presented by Carlsson and Kardomateas (2011). One of these theories which considers the compressibility of the core is called high order sandwich panel theory (HSAPT). HSAPT that was proposed and developed primarily by Frostig *et al*. (1992) is based on variational principle. In HSAPT the face sheets was model using classical beam/plate theory. HSAPT consider the transverse and shear stresses in the core but neglect the in-plane stresses. Gradually, the HSAPT theory was modified (Schwarts-Givli *et al*. 2007, Rabinovitch *et al*. 2003, Malekzadeh *et al*. 2006, Jedari Salami *et al*. 2014, Phan *et al*. 2011, Dariushi and Sadighi 2014). In improved high order sandwich panel theory (IHSAPT), first order shear deformation theory (FSDT) was accounted for the face sheets (Malekzadeh *et al*. 2006, Malekzadeh Fard 2014). Besides, the HSAPT developed with considering the in-plane rigidity of the core and proposed as extended high order sandwich panel theory (EHSAPT) (Phan *et al*. 2011). Although this theory has been used extensively to investigate the behavior of sandwich structures, a few literatures deal with modeling of impact response of sandwich structures with HSAPT (Malekzadeh *et al*. 2006, Malekzadeh Fard 2014, Yang and Qiao 2005, 2007).

Bennai *et al*. (2015) presented a new refined hyperbolic shear and normal deformation beam theory to study the free vibration and buckling of functionally graded (FG) sandwich beams under various boundary conditions. The effects of varying gradients, thickness stretching, boundary conditions, and thickness to length ratios are studied on the bending, free vibration and buckling of functionally graded sandwich beams.

High order impact model of sandwich structures with flexible core was first presented by Yang and Qiao (2005) and improved by Malekzade *et al*. (2006).

Yang and Qiao (2005) incorporated a foreign object impact process in the higher-order model and analyzed local deflection and stress concentration effects of the impact. The core was considered as a two dimensional elastic medium and the face sheets follow classical beam theory. Small strain hypothesis are adopted for the faces and the core. Three dynamic models were considered to predict free vibration of sandwich beams. The first model neglect the dynamic effect of the core (that is true for sandwich structures with low density core materials). The second model considers the dynamic effect of core but neglect the horizontal vibration and rotary inertia of the core and the face sheets and the third model considers the full dynamic effect. The second model was used to model the impact behavior. The governing equations were solved and the results were validated with LS-DYNA finite element simulation.

In another study, Yang and Qiao (2007) used the HSAPT to study vibration and impact behavior of large scale fiber reinforced polymer structural honey comb composite sandwich beams with sinusoidal core geometry. The validity of results is demonstrated by agreement with finite element simulations using ABAQUS and LS-DYNA for simulation of vibration and impact, respectively. Yang and Qiao (2007) also studied the effect of asymmetric lay up of sandwich beams with arbitrary boundary conditions. Finite difference method (FDM) is used to solve the governing equations. The effect of joint-joint supported and clamped boundaries and also load spreading on impact response is discussed. It has been concluded that high order impact sandwich panel with FDM is capable to accurately predict the impact response and the generated stress in a sandwich beam.

Malekzadeh *et al*. (2006) improved the model that has been proposed by Yang and Qiao (2005) by considering first order shear deformation theory (FSDT) for face sheets. Low velocity impact dynamic of a composite sandwich panel with transversely flexible core is analyzed and multiple small impactors with small masses is assumed. The kinematic relations for face sheets and core were based on small deformation and rotations. Also, the fully dynamic effects of all constituents are considered.

Khalili *et al*. (2007) studied the effects of important physical and geometrical parameters on low velocity impact behavior of composite sandwich panels with improved higher order sandwich panel theory (IHSAPT). It has been concluded that dynamic behavior of sandwich panel depends on various parameters such as the impact point, aspect ratio and length to thickness ratio of the panel, core thickness, boundary conditions and impactor weight and velocity.

Sohel *et al*. (2003) studied the behavior of steel-composite sandwich beams under low velocity hard impact. A series of tests was conducted to study damage characteristic and performance of sandwich beams with different spacing of shear connector. Spacing of shear connectors is found to have significant effects on the impact response of the beams.

In the present study a new nonlinear high order sandwich panel theory are introduced to predict the impact behavior of sandwich beams. The face sheets follow the Third order shear deformation beam theory (TSDT). The mathematical formulation adopts TSDT assumption for the face sheets provides zero transverse shear stress on the upper and lower surfaces as free edges of the sandwich panels. So, by introducing the new theory, one step closer to the exact elasticity solution. Considering that moderately large transverse deflection could be occurred under impact loading, nonlinear Von-Karman kinematic relations is carried out for strains of face sheets and the core. Two mentioned improvements have hitherto not applied in conventional EHSAPT for analyzing the sandwich panels under low velocity impact. The analytical results are validated with experimental results. A series of low-velocity impact tests were performed using a drop weight impact testing machine. Two groups of specimen with fibrous composite and aluminum face sheets were fabricated and tested.

(a) Description of the geometrical configuration

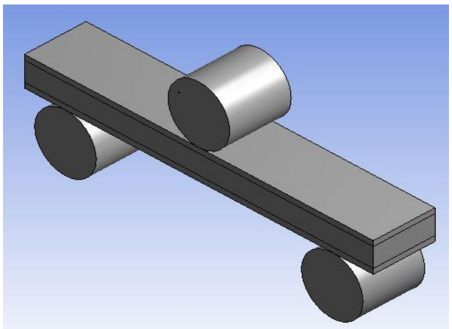

(b) Description of simply supports and cylindrical impactor

Fig. 1 A sandwich beam

2. Analytical formulation

A sandwich beam whose length, width, and total thickness are represented by *l*, *b*, and *d* is considered as it is shown in Fig. 1. The sandwich is formed from three parts: top and bottom face sheets and core layer. All parts are assumed with uniform thickness and the z coordinate of each part is measured downward from its mid-plane. The face sheets and the core made of materials characterized by linear elastic constitutive relations. Third-order shear deformation theory (TSDT) is applied in formulation of the face sheets. Also, geometrically nonlinear Von-Karman relations are taken into account to obtain strains.

2.1 Higher order theory for face sheets

The displacement components of the top and bottom face sheets are formulated based on third order shear deformable theory (Reddy 2006). Therefore, in- plane and transverse displacement components, i.e., u^i and w^i may be written in terms of in- plane displacements of mid-plane u^i_0 and transverse displacement of the mid-plane w^i_0, and φ^i rotations of cross sections about the *y* axes, as

$$\begin{aligned} u^i(x,z,t) &= u_0^i(x,t) + z_i\varphi^i(x,t) - C_s z_i^3(\varphi^i + w^i_{0,x}) \\ w^i(x,z,t) &= w_0^i(x,t) \end{aligned} \tag{1}$$

In which $C_s = 4/3h_i^2$ to consider quadratic variation of transverse shear strains and satisfy the vanishing of them on the top and bottom surfaces of the face sheets. Also ($i = t$ or b) superscript refers to top and bottom face sheets. Based on nonlinear Von-Karman kinematic relations

$$\varepsilon^i_{xx} = u^i_{0,x} + \frac{1}{2}\left(w^i_{0,x}\right)^2 + z\,\phi^i_{,x} - C_s z^3(\phi^i_{,x} + w^i_{0,xx}) \tag{2}$$

$$\gamma^i_{xz} = u^i_{,z} + w^i_{,x} = (1 - 3C_s z_i^2)(\varphi^i + w^i_{0,x}) \tag{3}$$

As the top and bottom face sheets are considered linear elastic laminates the stress- strain relations can be defined as

$$\begin{aligned} \sigma^i_{xx} &= \bar{C}_{11}\varepsilon^i_{xx} \\ \tau^i_{xz} &= \bar{C}_{55}\gamma^i_{xz} \end{aligned} \tag{4}$$

Where $\bar{C}_{11}$ and $\bar{C}_{55}$ are transformed stiffness coefficients, and

$$\begin{aligned} \bar{C}_{11} &= C_{11}(\cos(\theta))^4 + 2(C_{12} + C_{66})(\cos(\theta))^2(\sin(\theta))^2 \\ &\quad + C_{22}(\sin(\theta))^4 \\ \bar{C}_{55} &= C_{55}(\cos(\theta))^2 + C_{44}(\sin(\theta))^2 \end{aligned} \tag{5}$$

Where Θ is positive rotation of principal material axes from *x-y* axes, and C_{mn} (*m*, *n* = 1 to 6) are the stiffness coefficients in coordinates aligned with principal material directions. These coefficients, in terms of engineering constants, could be reduced from orthotropic one. Since the 2-3 plane is the plane of isotropy the 2 and 3 subscripts on the stiffness are interchangeable. Thus, stiffness coefficients are

$$\begin{aligned} C_{11} &= \frac{E_1(1 - \nu_{23}^2)}{\Delta} \\ C_{22} &= \frac{E_2(1 - \nu_{12}\nu_{21})}{\Delta} \\ C_{12} &= \frac{E_1(\nu_{21} + \nu_{21}\nu_{23})}{\Delta} \\ C_{44} &= G_{23}\,,\ C_{55} = G_{13}\,,\ C_{66} = G_{12} \\ \Delta &= 1 - 2\nu_{12}\nu_{21} - \nu_{23}^2 - 2\nu_{12}\nu_{21}\nu_{23} \end{aligned} \tag{6}$$

2.2 Core

The vertical and longitudinal displacements of core are assumed as cubic and quadratic polynomials in the transverse direction, respectively.

$$w^c(x,z,t) = w_0^c(x,t) + w_1^c(x,t)z_c + w_2^c(x,t)z_c^2 \tag{7}$$

$$\begin{aligned} u^c(x,z,t) = {} & u_0^c(x,t) + \varphi_0^c(x,t)z_c \\ & + u_2^c(x,t)z_c^2 + u_3^c(x,t)z_c^3 \end{aligned} \tag{8}$$

Where "*c*" superscript refers to core, "w_0" and "u_0" are the transverse and in-plane displacements; "φ_0" is the slope at the mid plane of the core about the y axes. In this study, the core is perfectly bonded to the face sheets. Hence, transverse and in-plane compatibility conditions in upper ($z = -c/2$), and lower ($z = c/2$) face sheet-core interfaces which can be obtained as follows

$$w^c(x,-\frac{c}{2},t) = w^t(x,\frac{h_t}{2},t) \tag{9}$$

$$u^c(x,-\frac{c}{2},t) = u^t(x,\frac{h_t}{2},t) \tag{10}$$

$$w^c(x,\frac{c}{2},t) = w^b(x,-\frac{h_b}{2},t) \tag{11}$$

$$u^c(x,\frac{c}{2},t) = u^b(x,-\frac{h_b}{2},t) \tag{12}$$

Using Eqs. (7)-(8) with Eqs. (9) to (12), the coefficients (w_1, w_2 and u_2, u_3) are analytically determined in terms of the displacement components of face sheets, mid plane displacement components and the slope at the mid plane of the core. Finally, after some algebraic manipulations the transverse and in-plane displacements of the core can be written as follow

$$\begin{aligned} w^c(x,z,t) &= w_0^c + \frac{1}{c}\left[w_0^b - w_0^t\right]z_c \\ &+ \frac{2}{c^2}\left[w_0^t + w_0^b - 2w_0^c\right]z_c^2 \end{aligned} \tag{13}$$

$$\begin{aligned} u^c(x,y,z,t) = {} & u_0^c + \varphi_0^c z_c \\ & + \left[\frac{2}{c^2}\left(u_0^t + u_0^b - 2u_0^c + \frac{h_t}{2}\varphi^t - \frac{h_b}{2}\varphi^b \right.\right. \\ & \left.\left. - \frac{h_t}{6}(\varphi^t + w_{0,x}^t) + \frac{h_b}{6}(\varphi^b + w_{0,x}^b)\right)\right] z_c^2 \\ & + \left[\frac{4}{c^3}\left(-u_0^t - \frac{h_t}{2}\varphi^t - \frac{h_b}{2}\varphi^b + u_0^b - c\varphi_0^c \right.\right. \\ & \left.\left. + \frac{h_t}{6}(\varphi^t + w_{0,x}^t) + \frac{h_b}{6}(\varphi^b + w_{0,x}^b)\right)\right] z_c^3 \end{aligned} \tag{14}$$

The Von-Karman strain-displacement relations for the core can be defined as

$$\varepsilon_{xx}^c = u_{,x}^c + \frac{1}{2}\left(w_{,x}^c\right)^2 \tag{15}$$

$$\varepsilon_{zz}^c = w_{,z}^c \tag{16}$$

$$\gamma_{xz}^c = u_{,z}^c + w_{,x}^c \tag{17}$$

Applying Eqs. (13)-(14) into Eqs. (15) to (17), the strain-displacement relations based on independent variables can be obtained. The stress- strain relationships for the orthotropic core can be read as follows

$$\begin{bmatrix} \sigma_{xx}^c \\ \sigma_{zz}^c \\ \tau_{xz}^c \end{bmatrix} = \begin{bmatrix} c_{11} & c_{13} & 0 \\ c_{13} & c_{33} & 0 \\ 0 & 0 & c_{55} \end{bmatrix} \begin{bmatrix} \varepsilon_{xx}^c \\ \varepsilon_{zz}^c \\ \gamma_{xz}^c \end{bmatrix} \tag{18}$$

Where C_{mn} are the stiffness coefficients. By substituting the strain-displacement relations in Eq. (18) the stresses are expressed through displacements.

2.3 Dynamics of contact region

The impact load applied by a spherical impactor may be related to the indentation value of the top face sheet through the following contact law (Abrate 2005)

$$F(t) = K_h \alpha^n \tag{19}$$

Where α is the indentation value between the impactor and the top face sheet. Therefore, it is defined as

$$\alpha = w_p - w^t(x_0,-\frac{h_t}{2},t) \tag{20}$$

Where w_p indicates the displacement of impactor, and $w^t(x,-h_t/2,t)$ is the transverse displacement of the top face sheet at the impact position. Natural logarithm of Eq. (19) yields

$$\ln(F) = n\ln(\alpha) + \ln(k_h) \tag{21}$$

An experimental indentation test on a fully backed sandwich plate, shows the relation between force (F) and indentation (α). When the (F-α) cure is plotted in logarithmic coordinate system, the slope and y-intercept of line indicates (n) and Ln (k), respectively

2.4 Governing equations

The Ritz method is pursued to obtain governing equations of motion from total potential energy function of the sandwich plate. The total potential energy (Π) includes kinetic energy (T), strain energy (U) and potential of external works (W).

$$\prod = T + U + W \tag{22}$$

The strain energy of the sandwich beam that consists of stress and strain of face sheets and core, is given by

$$\begin{aligned} U = {} & \int_{V_t}\left(\frac{1}{2}\sigma_{xx}^t\varepsilon_{xx}^t + + \frac{1}{2}\tau_{xz}^t\gamma_{xz}^t\right)dv_t \\ & + \int_{V_c}\left(\frac{1}{2}\sigma_{xx}^c\varepsilon_{xx}^c + \frac{1}{2}\sigma_{zz}^c\varepsilon_{zz}^c + \frac{1}{2}\tau_{xz}^c\gamma_{xz}^c\right)dv_c \\ & + \int_{V_b}\left(\frac{1}{2}\sigma_{xx}^b\varepsilon_{xx}^b + \frac{1}{2}\tau_{xz}^b\gamma_{xz}^b\right)dv_b \end{aligned} \tag{23}$$

The kinetic energy of the system, considering both the kinetic energies of the sandwich panel and impactor. Thus, it can be written as

$$\begin{aligned} T = {} & \int_{V_t}\left(\frac{1}{2}\rho_t(\dot{u}_t^2 + \dot{w}_t^2)\right)dv_t + \int_{V_c}\left(\frac{1}{2}\rho_c(\dot{u}_c^2 + \dot{w}_c^2)\right)dv_c \\ & + \int_{V_b}\left(\frac{1}{2}\rho_b(\dot{u}_b^2 + \dot{w}_b^2)\right)dv_b + \frac{1}{2}M_p\dot{w}_P^2 \end{aligned} \tag{24}$$

Where ρ_t, ρ_b and ρ_c are the densities of the top face sheet, bottom face sheet and the core, respectively. Also, M_P indicates the mass of the impactor. The potential of external works equals to

$$W = -\int_0^t F(t)\,\mathrm{d}w_0 \tag{25}$$

Using Ritz method, the solution of the displacement variables should be assumed based on satisfying the essential boundary conditions. Thus, in case of simply supported beam, displacement functions of the face sheets and the core can be expressed in the following forms. Where Ω^i, represents the time dependent unknown coefficients according to assumed displacement functions. M is the number of terms should be selected to assure the convergence of the series functions.

$$\begin{gathered}\left\{\Omega^i(t)\right\} = \left\{\left\{U_m^i(t)\right\}, \left\{\Phi_m^i(t)\right\}, \left\{W_m^i(t)\right\},\right\} \\ i = t, b, c, m = 1 \ldots M\end{gathered} \tag{26}$$

$$q^i(x,t) = R_\delta \sum_{m=1}^{M} \Omega_m^i(t)\, \mathrm{P}_m(\xi) \tag{27}$$

$$P_m(x) = \cos[(j-1)\arccos(x)] \tag{28}$$

In this study Chebyshev polynomial (Upadhyay and Shukla 2013) type of shape functions are used. Here $P_m(\zeta)$ is one dimensional Chebyshev polynomial and R_δ are the functions that have to be chosen according to the essential boundary conditions. So, the functions can be written as Eqs. (29) and (30) for simply supported and clamped beam, respectively

$$R_\delta = 1 - \xi^2 \quad , (\delta = w_0^i(\mathrm{x,t})) \tag{29}$$

$$R_\delta = 1 - \xi^2 \quad , (\delta = u_0^i(\mathrm{x,t}), w_0^i(\mathrm{x,t}), \varphi_0^i(\mathrm{x,t})) \tag{30}$$

Superscript i may denotes the top or bottom face sheets and the core. Substituting the Eq. (27) in to Eqs. (23) to (25) eliminates the dependency of the unknown variables to the spatial coordinates. Equations of motions then can be deduced based on the applying generalized Lagrange equations, as follows

$$\frac{\partial \Pi}{\partial \Omega_i} = 0 \Rightarrow \frac{d}{dt}\left(\frac{\partial T}{\partial \dot{\Omega}_i}\right) + \frac{\partial U}{\partial \Omega_i} = -\frac{\partial W}{\partial \Omega_i} \tag{31}$$

The resulted equations from Eq. (31) are a system of nonlinear coupled ordinary differential equations. The set of equations in a matrix form, can be written as the follows

$$[M]\left\{\ddot{\Omega}\right\} + [K]\{\Omega\} = \{F\} \tag{32}$$

Where $[M]$ is mass matrix, $[K]$ is a nonlinear coefficient matrix (or stiffness matrix) that depends upon unknown coefficients Ω^i, $[F]$ is the force vector. The resulted nonlinear second order differential equations are then solved by the fourth-order Rung- Kutta method. The initial conditions for system of equations are as follows

$$\begin{cases}\Omega(t=0) = [0] \\ w_P(t=0) = 0, \dot{w}_P(t=0) = V_0\end{cases} \tag{33}$$

3. Experimental procedure

Low velocity impact tests were carried out on two groups of sandwich beams with composite and aluminium face sheets. Fibrous composite face sheets were glass/epoxy (0-90-90-0-0-90-90-0) symmetric laminates with 1.2 mm thickness. The materials used for manufacturing of specimens were aluminum2024-T3 sheets with 1.2 mm thicknesses, unidirectional S2 glass/ FM94-epoxy prepreg and ECA Nomex honeycomb (cell size = 3.2 mm) from Euro-composites. Nomex core thickness was 10 mm for all specimens.

At first, composite face sheets were made by hand lay-up and were cured in autoclave for 3 hours at 6 bar pressure in temperature 120℃. The Face sheets (Aluminium and composite) were bonded to Nomex core with FM-94 Adhesive layers and cured in autoclave for 1 hour under 2 bar in 120℃. Large panels were manufactured and then small specimens were cut in rectangular shape with 170 mm side length. Notations, stacking sequence and thickness of each specimen are presented in Table 2.

Low velocity impact testes were carried out at the centre of simply supported specimens using instrumented drop weight tower (Fig. 2). The span length of specimens was 130 mm and the velocity of impactor nose was measured by two laser sensors with known distance. Impactor weight was constant (1000 gr) for all tests, therefore height of impactor controlled the impact velocity. A cylindrical steel impactor with 8 mm radius was used. At least five specimen for each reported result were tested.

The elastic material properties of all components that have been used for manufacturing the specimens are tabulated in Table 2.

Table 1 Sequencing and geometry of specimens

Specimen	Face sheets	Core	Core thickness (mm)	Face sheet thickness (mm)	Beam length (mm)
A	Aluminum	ECA Nomex	10	1.2	170
B	Glass/Epoxy	ECA Nomex	10	1.2	170

Table 2 Material properties

Material	Young's modulus [GPa]	Shear modulus [GPa]	Poisson's ratio	Density [Kg/m^3]
Aluminum	E = 70.15	G = 26.3	υ = 0.33	ρ = 2780
S2 glass/ FM94-epoxy prepreg	E_1 = 48.9, E_2 = 5.5, E_3 = 5.5	G_{12} = 5.5, G_{13} = 5.5, G_{23} = 5	υ_{12} = 0.33, υ_{13} = 0.33, υ_{23} = 0.0371	ρ = 2000
ECA Honeycomb	E_T = 0.295, E_L = 0.0455, E_W = 0.005	G_{12} = 0.065, G_{23} = 0.023	υ_{31} = 0.27, υ_{32} = 0.4	ρ = 144

(a) Tower of drop weight apparatus (b) Impactor and specimen

Fig. 2 Low velocity impact test on sandwich beam

4. Results and discussion

In this section, the numerical results based on above procedure are presented to study impact response of a sandwich beam with glass/epoxy composite face sheets and Nomex honeycomb cores. At first, comparison study is performed. Afterward parametric studies are carried out to examine the influences of involved parameters.

4.1 Comparison study

To validate the accuracy and effectiveness of the present method, results of present theory are validated by comparing the predicted results for a sandwich beam subjected to low velocity impact with the experimental results. Two cases of face sheets are made from aluminium and laminated composite for the simply supported sandwich beams with Nomex honeycomb cores are carried out in comparison studies. The sandwich beams are subjected by a rigid impactor with two initial velocities are considered. The contact force histories obtained from present theory are compared with experimental results are given in Fig. 3. The main reasons of difference may be the present contact force model, omitting the friction between supporters and specimens, ignoring the cohesive layers between face sheets and core and many defects occurred during fabrication process that are not considered in theoretical formulation. Besides, the time histories of displacement of the impactor for both types of specimens obtained by twice integration from experimental acceleration data are compared with those computed from theoretical ones in Fig. 4. It is seen that, the comparison is well justified which proofs the accuracy and efficiency of the developed method.

4.2 Parametric studies

Low velocity impact characteristics of sandwich beams with laminated composite face sheets and Nomex honeycomb core are studied. The face sheets stacking sequence are symmetric cross-ply (0/90/90/0/0/90/90/0) by considering 0.15 mm lamina thickness. The material properties of Nomex honeycomb core, aluminium and laminated composite face sheets are given in Table 2.

Geometrical characteristics of the sandwich beam are length L = 130 mm, width b = 30 mm and thickness of the face sheets $h_t = h_b$ = 1.2 mm. In this study, the thickness of the face sheets are kept constant and height of the core is adjusted so that the core-to-face sheet thickness ratio are C/h_t = 4, 6 and 8. Impactor is made from steel with material properties E_s = 207 GPa, ρ_s = 7960 kg/m^3 and υ_s = 0.5. Unless otherwise stated, a cylindrical impactor with radius R_{imp} = 15 mm and initial velocity V_{imp} = 2 m/s is impacting the target at the mid-span of the beam, i.e., $x_{imp} = L/2$. In the next, sandwich beams with both edges simply supported is analysed since generally the required time for the stress wave to travel to boundary and reflect back is less than the low velocity impact event time. After examining the validity of the present solution, the effects of boundary

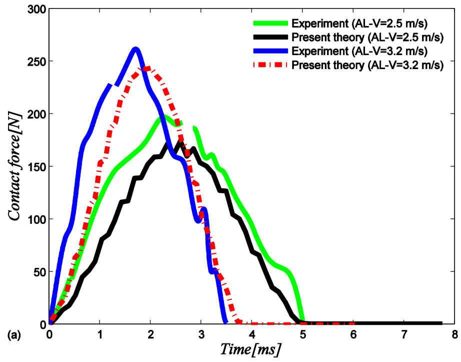

(a) Aluminium face sheets (experimental smooth data)

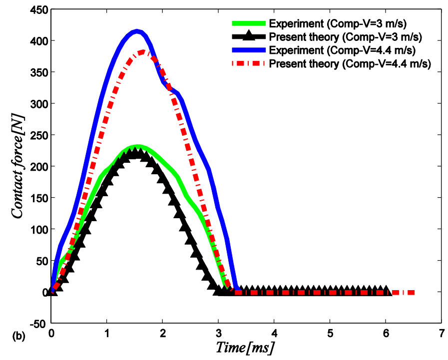

(b) Laminated composite face sheets (experimental smooth data)

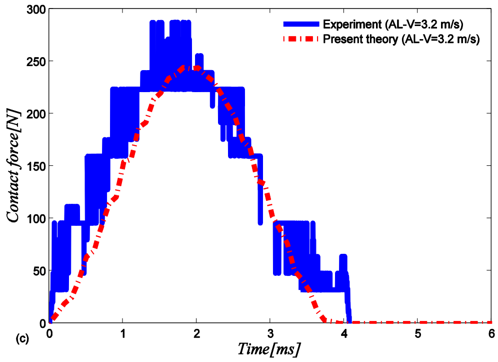

(c) Aluminium face sheets (experimental raw data)

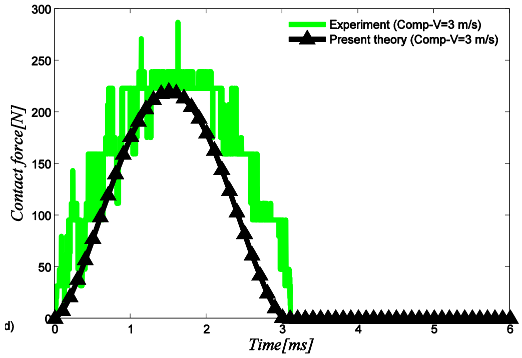

(d) Laminated composite face sheets (experimental raw data)

Fig. 3 A comparison on contact force history of simply supported sandwich beam with Nomex honeycomb core

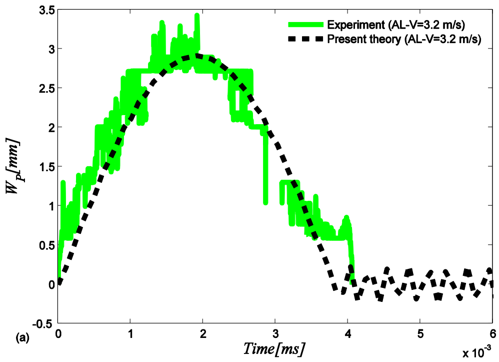

(a) Aluminium face sheets

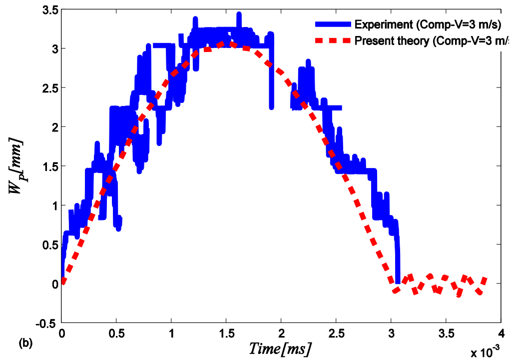

(b) Laminated composite face sheets

Fig. 4 A comparison on displacement of impactor history of simply supported sandwich beam with Nomex honeycomb core

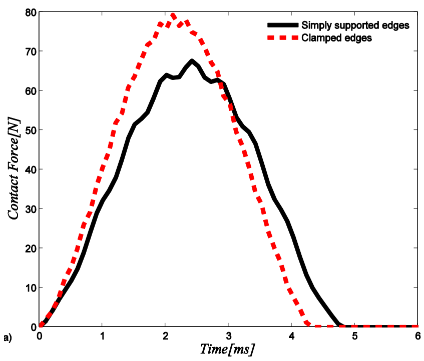

(a) Contact force history

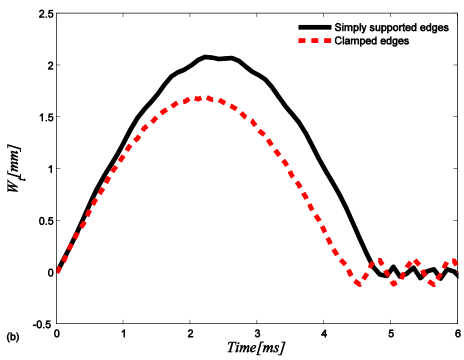

(b) Central transverse displacement

Fig. 5 The effect of boundary conditions on low velocity impact responses at the midspan point of the top face

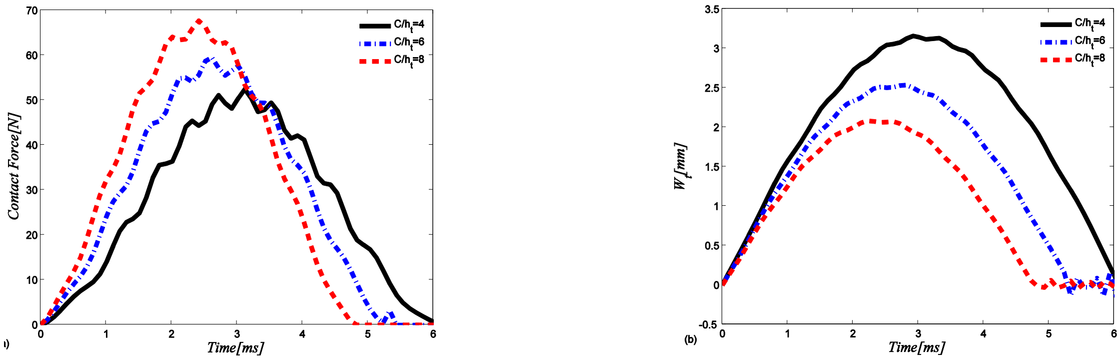

(a) Contact force history (b) Central transverse displacement

Fig. 6 The effect of core to face sheet thickness ratio on low velocity impact responses at the midspan point of the top face

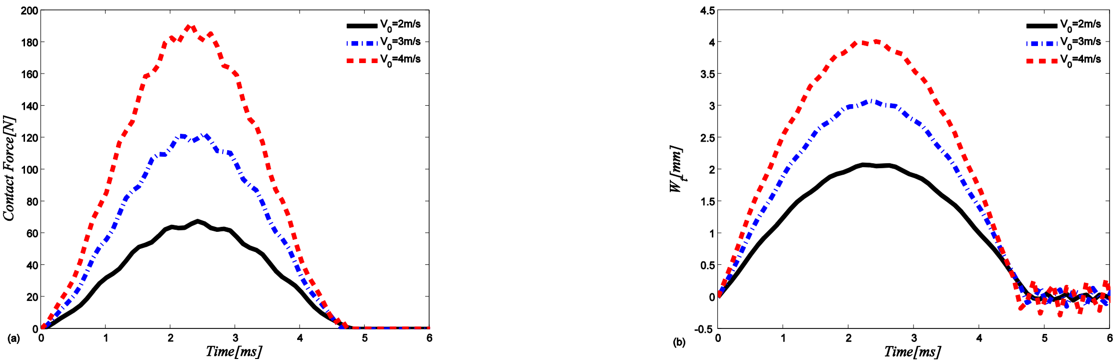

(a) Contact force history (b) Central transverse displacement

Fig. 7 Influence of the impactor initial velocity on low velocity impact responses at the midspan of the top face

conditions, core-to-face sheet thickness ratio, initial velocity of the impactor, the impactor mass and position of the impactor are studied in detail.

4.2.1 Case I: Effect of boundary conditions

To assess influence of the boundary conditions, the contact force history characteristics and the central transverse displacement of top face sheet for simply supported sandwich beam are depicted in Fig. 5. It is observed that peak contact force is maximum for immovable clamped beam, whereas the highest lateral deflection of the beam belongs to simply supported one. Such trend is interpreted based on the higher local flexural rigidity of the immovable clamped edge in comparison to a simply supported one.

4.2.2 Case II: Effect of the core-to-face sheet thickness ratio (c/h_t)

The effect of core-to-face sheet thickness ratio (c/h_t) on the low velocity response of the simply supported sandwich beam is indicated in Fig. 6. It can be seen from Fig. 5 that the sandwich beam with higher core-to-face sheet thickness ratio has lower transverse displacement along with higher contact force. Since the thickness of the face sheets are kept constant, therefore, the increasing c/h_t involving thicker cores. As thicker core is, the higher the flexural stiffness of the sandwich panel is. So, with the increase of c/h_t, the flexural stiffness of sandwich panel becomes higher and in turn, the contact force increases. According to the same reasoning, transverse displacement of the top face sheet is smaller at the impacted section of the top face sheet.

4.2.3 Case III: Influence of Initial Velocity of Impactor

The effect of the initial kinetic energy of the impactor includes both the mass and initial velocity of the impactor. This task is accomplished through two different ways: increasing the mass of the indenter while fixing value of the initial velocity and vice versa. Effects of initial velocity of the impactor on the low velocity impact characteristics of the simply supported sandwich beam is analysed in this section. Geometry of the sandwich beam and impactor are the same with those used in the previous section. A simply supported sandwich beam is considered where core-to-face sheet thickness ratio is c/h_t = 8. Contact force history and transverse displacement of the top face sheet are provided in Fig. 7. As seen from this figure, an increase in the initial velocity of the impactor, which results in higher initial energy of the system, higher peak contact force are concluded. The influence of initial velocity of the impactor is much more pronounced on the peak contact force than the contact time. Moreover, the central transverse displacement of the top face sheet increases as the initial velocity of the impactor increases.

4.2.4 Case IV: Impactor mass effect

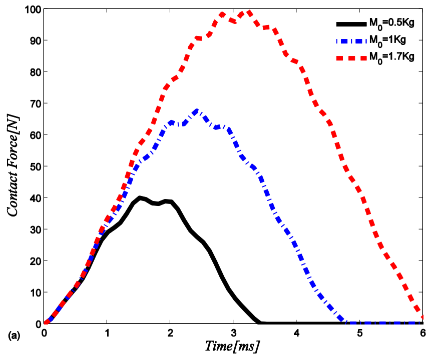

(a) Contact force history

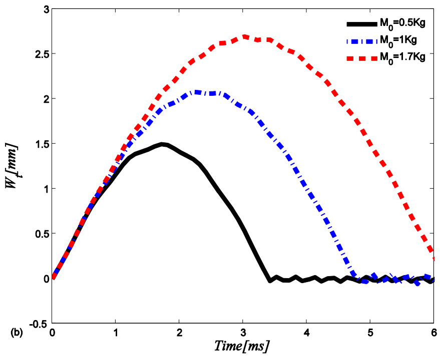

(b) Central transverse displacement

Fig. 8 Influence of the impactor mass on low velocity impact responses at the midspan point of the top face

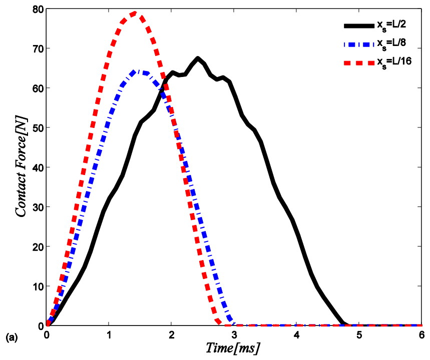

(a) Contact force history

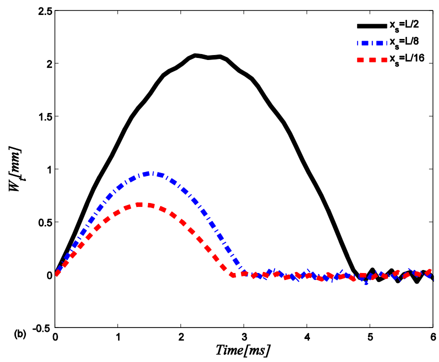

(b) Central transverse displacement

Fig. 9 The influence of impactor position on contact force and deflection histories of the top face sheet

The effect of projectile mass is investigated herein. All parameters of the system are the same with those used in previous section. A S-S sandwich beam with soft core where core-to-face sheet thickness ratio $c/h_t = 8$ is considered. Initial velocity of the impactor is chosen as $V_{imp} = 2$ m/s. In addition to $M_0 = 1$ Kg, two other cases of $M_0 = 0.5$ Kg and $M_0 = 1.7$ Kg are considered. Since the impactor mass is the only variable, its influence on the dynamic response can be predicted in Fig. 7. As seen from this figure, an increase in the impactor mass leads to the higher contact force and also higher contact time. Moreover, central displacement of the top face sheet increase as the impactor mass increases.

As expected, results depicted in Figs. 7 and 8 reveal that as the initial kinetic energy of the impactor increases, the contact forces and central displacement of the top face sheet increase. However, if the increase in the kinetic energy of the impactor has occurred due to an increased impactor mass, the contact time will be higher otherwise it will be lower in comparison the initial contact time.

4.2.5 Case V: Effect of impactor position

To investigate the effect of the impactor position, an immovable clamped sandwich beam under the impact of a rigid mass is considered. Geometry of the impactor and beam are the same with the previous section. Results are presented in Fig. 9. In this figure, the contact force history and deflection of the top face sheet are depicted for three cases of impactor positions, that are $x_s = L/2$, $L/8$ and $L/16$. As results show, due to the higher local bending rigidity in the neighbourhood of the clamped edge of the beam, the contact force increases, whereas the lateral deflection of the top face sheet decreases.

5. Conclusions

In this study, response of sandwich beam with laminated composite and aluminium face sheets and Nomex honeycomb cores subjected to the action of an impacting mass based on the EHSAPT is presented. Contact force between the impactor and the beam is obtained using the modified Hertz law. In this theory, the nonlinear Von Karman type relations for strains of face sheets and the core are adopted. The face sheets follow the third order shear deformation beam theory (TSDT). Besides, the two dimensional elasticity is used for the core. The field equations are derived via the Ritz based applied to the total energy of the system. The solution is obtained in the time domain by implementing the fourth order Runge-Kutta method. Numerical results are provided to explain the influences of various parameters such as the effects of core-to-face sheet thickness ratio, initial velocity of the impactor, the impactor mass and position of the impactor. Generally, the numerical results based on the extended high order sandwich panel theory reveal that:

- Based on boundary condition effect, peak contact force is maximum for immovable clamped beam, whereas the highest lateral deflection of the beam belongs to simply supported one. Such trend is interpreted based on the higher local flexural rigidity of the immovable clamped edge in comparison to the simply supported one.
- The sandwich beam with higher core-to-face sheet thickness ratio has lower transverse displacement along with higher contact force.
- An increase in the initial velocity of the impactor, which results in higher initial energy of the system, higher peak contact force are concluded. The influence of initial velocity of the impactor is much more pronounced on the peak contact force than the contact time.
- An increase in the impactor mass leads to the higher contact force and also higher contact time. Moreover, central displacement of the top face sheet increase as the impactor mass increases. Also, if the increase in the kinetic energy of the impactor has occurred due to an increased impactor mass, the contact time will be higher otherwise it will be lower in comparison the initial contact time.
- It could be concluded that if the impact position is closer to clamped edges, the contact force increases, whereas the lateral deflection of the top face sheet decreases due to the higher local bending rigidity in the neighbourhood.
- Generally, It is found that each of these parameters have significant effect on the impact characteristics which should be considered.

Acknowledgments

This work supported by Research Program supported by the Islamic Azad University, Damavand branch, Iran.

References

Abrate, S. (2005), *Impact on Composite Structures*, Cambridge University Press, New York, NY, USA.

Abrate, S. and Di Sciuva, M. (2017), “Equivalent single layer theories for composite and sandwich structures: A review”, *Compos. Struct.*, **179**, 482-494.

Benbakhti, A., Bouiadjra, M.B., Retiel, N. and and Tounsi, A. (2016), “A new five unknown quasi-3D type HSDT for thermomechanical bending analysis of FGM sandwich plates”, *Steel Compos. Struct., Int. J.*, **22**(5), 975-999.

Bennai, R., Ait Atmane, H. and Tounsi, A. (2015), “A new higher-order shear and normal deformation theory for functionally graded sandwich beams”, *Steel Compos. Struct., Int. J.*, **19**(3), 521-546.

Caliri, M., Ferreira, A. and Tita, V. (2016), “A review on plate and shell theories for laminated and sandwich structures highlighting the Finite Element Method” *Compos. Struct.*, **156**, 63-77.

Carlsson, L.A. and Kardomateas, G.A. (2011), *Structural and Failure Mechanics of Sandwich Composites*, Springer, New York, NY, USA.

Daniel, I.M., Gdoutos, E.E. and Rajapakse, Y.D.S. (2009), *Major Accomplishments in Composite Materials and Sandwich Structures*, Springer, New York, NY, USA.

Dariushi, S. and Sadighi, M. (2014), “A new nonlinear high order theory for sandwich beam: an analytical and experimental investigation”, *Compos. Struct.*, **108**, 779-788.

Frostig, Y., Baruch, M., Vilnay, O. and Sheinman, I. (1992), “High order theory for sandwich beam behavior with transversely flexible core”, *J. Eng. Mech.*, **118**(5), 1026-1043.

Ganapathi, S.C., Peter, J.A., Lakshmanan, N. and Iyer, N.R. (2016), “Behavior of light weight sandwich panels under out of plane bending loading”, *Steel Compos. Struct., Int. J.*, **21**(4), 775-789.

Jedari Salami, S., Sadighi, M. and Shakeri, M. (2014), “Improved extended high orderanalysis of sandwich beams with a bilinear core shear behaviour”, *J. Sandw. Struct. Mater.*, **16**(6), 633-668.

Khalili, M.R., Malekzadeh, K. and Mittal, R.K. (2007), “Effect of physical and geometrical parameters on transverse low-velocity impact response of sandwich panels with a transversely flexible core”, *Compos. Struct.*, **77**(4), 430-443.

Liu, J., Zhu, X., Li, T., Zhou, Z., Wu, L. and Ma, L. (2014), “Experimental study on the low velocity impact responses of all-composite pyramidal truss core sandwich panel after high temperature exposure”, *Compos. Struct.*, **116**, 670-681.

Malekzadeh Fard, K. (2014), “Higher order impact analysis of sandwich panels with functionally graded flexible cores” *Steel Compos. Struct., Int. J.*, **16**(4), 389-415.

Malekzadeh, K., Khalili, M.R., Olsson, R. and Jafari, A. (2006), “Higher-order dynamic response of composite sandwich panels with flexible core under simultaneous low-velocity impacts of multiple small masses”, *Int. J. Solids Struct.*, **43**(22-23), 6667-6687.

Noor, A.K., Burton, W.S. and Bert, C.W. (1996), “Computational models for sandwich panels and shells”, *Appl. Mech. Rev.*, **49**(3), 155-199.

Phan, C., Kardomateas, G.A. and Frostig, Y. (2011), “Analysis of sandwich beams with a compliant core and with in-plane rigidity-extended high-order sandwich panel theory versus elasticity”, *J. Appl. Mech.*, **79**(4), 1-11.

Qiao, P. and Yang, M. (2007), “Impact analysis of fiber reinforced polymer honeycomb composite sandwich beams”, *Compos. Part B*, **38**(5-6), 739-750.

Rabinovitch, O., Vinson, J.R. and Frostig, Y. (2003), “High-order analysis of unidirectional sandwich panels with piezolaminated face sheets and soft core”, *AIAA*, **41**(1), 110-118.

Rajaneesh, A., Sridhar, I. and Rajendran, S. (2014), “Relative performance of metal and polymeric foam sandwich plates under low velocity impact”, *Int. J. Impact Eng.*, **65**, 126-136.

Reddy, J.N. (2006), *Theory and Analysis of Elastic Plates and Shells*, CRC Press, London, UK.

Reddy, B.G.V. and Sharma, K.V. (2014), “Deformation and impact energy absorption of cellular sandwich panels”, *Mater. Des.*, **61**, 217-227.

Schwarts-Givli, H., Rabinovitch, O. and Frostig, Y. (2007), “High-order nonlinear contact effects in the dynamic behavior of delaminated sandwich panels with a flexible core”, *Int. J. Solids Struct.*, **44**(1), 77-99.

Sohel, K.M.A., Richard Liew, J.Y., Alwis, W.A.M. and Paramasivam, P. (2003), “Experimental investigation of low-velocity impact characteristics of steel-concrete-steel sandwich beams”, *Steel Compos. Struct., Int. J.*, **3**(4), 289-306.

Stocchi, A., Colabella, L., Cisilino, A. and Alvarez, V. (2014), “Manufacturing and testing of a sandwich panel honeycomb core reinforced with natural-fiber fabrics”, *Mater. Des.*, **55**, 394-403.

St-Pierre, L., Deshpande, V.S. and Fleck, N.A. (2015), “The low velocity impact response of sandwich beams with a corrugated core or a Y-frame core”, *Int. J. Mech. Sci.*, **91**, 71-80.

Upadhyay, A.K. and Shukla, K.K. (2013), “Non-linear static and dynamic analysis of skew sandwich plates", *Compos. Struct.*, **105**, 141-148.

Yan, C. and Song, X. (2016), "Effects of foam core density and face-sheet thickness on the mechanical properties of aluminum foam sandwich", *Steel Compos. Struct., Int. J.*, **21**(5), 1145-1156.

Yang, M. and Qiao, P. (2005), "Higher-order impact modeling of sandwich structures with flexible core", *Int. J. Solids Struct.*, **42**(20), 5460-5490.

Yang, M. and Qiao, P. (2007), "Impact and damage prediction of sandwich beams with flexible core considering arbitrary boundary effects", *J. Sandw. Struct. Mater.*, **9**(5), 411-444.

Zenkert, D. (1995), *An Introduction to Sandwich Construction*, Engineering Materials Advisory Services, New York, NY, USA.

CC